RESEARCH MEMORANDUM

USE OF TRUNCATED FLAPPED AIRFOILS FOR IMPINGEMENT AND ICING TESTS OF FULL-SCALE LEADING-EDGE SECTIONS

By Uwe H. von Glahn

Lewis Flight Propulsion Laboratory
Cleveland, Ohio

NATIONAL ADVISORY COMMITTEE
FOR AERONAUTICS

WASHINGTON
July 24, 1956

NATIONAL ADVISORY COMMITTEE FOR AERONAUTICS

RESEARCH MEMORANDUM

USE OF TRUNCATED FLAPPED AIRFOILS FOR IMPINGEMENT AND ICING TESTS OF FULL-SCALE LEADING-EDGE SECTIONS

By Uwe H. von Glahn

SUMMARY

In an effort to increase the operational range of existing small icing tunnels, the use of truncated airfoil sections has been suggested. With truncated airfoils, large-scale or even full-scale wing-icing-protection systems could be evaluated. Therefore, experimental studies were conducted in the NACA Lewis laboratory icing tunnel with an NACA 65_1-212 airfoil section to determine the effect of truncating the airfoil chord on velocity distribution and impingement characteristics. A 6-foot-chord airfoil was cut successively at the 50- and 30-percent-chord stations to produce the truncated airfoil sections, which were equipped with trailing-edge flaps that were used to alter the flow field about the truncated sections. The study was conducted at geometric angles of attack of 0° and 4°, an airspeed of about 156 knots, and volume-median droplet sizes of 11.5 and 18.6 microns. A dye-tracer technique was used in the impingement studies.

With the trailing-edge flap on the truncated airfoil deflected so that the local velocity distribution in the impingement region was substantially the same as that for the full-chord airfoil, the local impingement rates and the limits of impingement for the truncated and full-chord airfoils were the same. In general, truncating the airfoils with flaps undeflected resulted in a substantially altered velocity distribution and local impingement rates compared with those of the full-chord airfoil. The use of flapped truncated airfoils may permit impingement and icing studies to be conducted with full-scale leading-edge sections, ranging in size from tip to root sections.

INTRODUCTION

The evaluation in wind tunnels of heat transfer and impingement characteristics of full-scale aircraft components in icing conditions has been limited by the relative size of the component and the test facility. Full-scale models avoid the complication of scaling gas-heated

passages, electric heating pads, skin thickness, and so forth. The size of the available icing tunnels, however, limits full-scale tests to smaller components such as wing tips and small radomes. Therefore, it is necessary to extrapolate data, often by questionable techniques, for such full-scale components as wing root sections and large nose radomes. The alternative is to conduct flight tests on the prototype aircraft in icing conditions. This latter method is costly in time and funds as well as in the necessary "retrofit" work if major system changes are required.

The simultaneous scaling of heat-transfer, impingement, and possibly icing characteristics (in the case of a cyclic de-icing system) presents formidable scale problems. Model-scale theories have been proposed (refs. 1 and 2) whereby a component could be completely scaled and tested under icing conditions equivalent to full-scale tests. The construction and instrumentation of such a scaled model, however, present many problems. Furthermore, the ability to obtain specified combinations of airspeed, water content, heating flux, and droplet size necessary for testing these scaled models is not readily achievable with present icing-tunnel equipment. Much setup and preliminary calibration effort would be required to meet the scale needs for models of various airframe or engine components. In addition, some icing-protection systems, notably cyclic de-icing systems, are difficult to test under scaled conditions because of inadequate means of simultaneously extrapolating conditions of impingement, ice-formation buildup, aerodynamic forces on an ice formation, and heat transfer from full-scale to model conditions. The problem imposed by local Reynolds number differences betweeen scaled and full-scale models must also be considered in heat-transfer studies.

In an effort to study and evaluate full-scale icing-protection systems for wing sections, some investigators have advocated the use of truncated airfoil models. These models utilize a full-scale leading-edge section followed by a faired section that, in effect, reduces the overall length or chord of the model. This procedure has definite merit since full-scale test conditions (within the capabilities of the research facility) conceivably could be obtained. The effect, however, of truncating the airfoil on impingement and heat-transfer parameters is not known. Truncating an airfoil will distort the flow field about the airfoil from that about the full-chord airfoil because the circulation about a truncated airfoil will not be the same as that for the full-chord airfoil. Consequently, full-scale impingement and heat-transfer relations would not be achieved with such a truncated airfoil.

Consideration of the circulation and flow-field problem suggested the use of a flap, either mechanical or jet, which by proper deflection could aid in restoring the circulation and, hence, flow field about the leading-edge region of the truncated airfoil to that for the full-chord airfoil. With such a possible restoration of the flow field about a

truncated airfoil equipped with a flap, a problem then arises whether the local impingement characteristics are also restored or whether they are influenced by the actual physical size of the full chord of the airfoil.

Therefore, a brief study was conducted at the NACA Lewis laboratory icing tunnel to determine the effect of the flow-field and impingement characteristics of NACA 65_1-212 airfoil sections made by truncating the airfoil. The effect on the flow field of truncating the airfoil were determined by measurement of the local velocity distribution over the models. Impingement data for all airfoil sections were obtained experimentally by the dye-tracer technique described in reference 3. The studies were made with and without deflection of a mechanical flap. The data from the truncated airfoil models are compared with those from a full-chord model.

SYMBOLS

The following symbols are used in this report:

A_s area of blotter segment, sq ft

b volume of water used to dissolve dye from blotter segments, ml

c percent concentration by weight of dye in water solution used in spray system

K_0 modified inertia parameter (ref. 3)

P true concentration of solution obtained from blotter segments, mg dye/ml solution

s surface distance measured from zero-chord point at leading edge, in.

t exposure time of blotter to spray cloud, sec

U local air velocity over airfoil surface, ft/sec

V_0 free-stream air velocity, ft/sec

$\overline{W}_\beta$ local water impingement rate obtained with droplet-size distribution in tunnel spray cloud, lb/(hr)(sq ft)

δ flap angle, deg

APPARATUS

Models

The initial model consisted of a wooden NACA 65_1-212 airfoil section of 6-foot chord spanning the 6-foot height of the icing tunnel (fig. 1). For the truncated models, the airfoil was successively cut in a spanwise plane approximately 36 and 22 inches from the leading edge (fig. 2(a)), corresponding to about the 50- and the 30-percent-chord stations, respectively. Hereinafter, the models will be referred to as the full-chord, the 50-percent-chord, and the 30-percent-chord airfoils. A manually adjustable metal trailing-edge flap about a foot long was attached to each of the truncated airfoils (fig. 2). The simple flap consisted of four metal plates hinged at three points, as shown in figure 2(b). The flap plate on the upper surface of the airfoil was slotted so that loosening of the attachment screws permitted a chordwise movement of the flap plate. The flap plate on the lower surface of the airfoil was fixed to the airfoil at the hinge line. When the flap plate attached to the upper surface of the airfoil was moved in a rearward direction, the flap deflected (fig. 2(b)). By definition, zero deflection of the flap occurred when the trailing edge of the flap coincided with the airfoil chord line. A maximum flap deflection of 20° from the chord line could be obtained for the 50-percent-chord airfoil and 22° for the 30-percent-chord airfoil. Installation of a flapped truncated airfoil in the icing tunnel is shown in figure 3.

Pressure belts were cemented to the wooden leading-edge region of all models to determine the pressure and velocity distribution over the airfoils. All pressure data were recorded photographically from multitube manometer boards.

Spray

A dyed-water spray cloud was provided by eight air-water atomizing nozzles located in the quieting chamber of the tunnel test section (ref. 3). The dyed-water solution contained an azo Carmoisine BA dye (red) of 1 percent by weight. The spray was turned on and off by fast-acting solenoid valves, while the spray duration was set and recorded with an electric timer. Further details of the spray system are described in reference 3.

PROCEDURE

Velocity Distribution

The velocity distributions for all airfoils were obtained at angles of attack of 0° and 4° and at an airspeed of about 156 knots. For the

truncated airfoils, the velocity distributions were obtained with the flap undeflected and deflected. With the flap deflected, the flap angle was changed until the velocity distribution over the leading-edge region of the truncated airfoils was substantially the same in the impingement region as that over the full-chord airfoil. The velocity-distribution data were not corrected for tunnel-wall interference effects.

Impingement

The impingement characteristics of the airfoils were studied by means of the dye-tracer technique (ref. 3) over the same range of conditions as those used in the velocity distribution studies. In the dye-tracer technique, water treated with known small amounts of the water-soluble dye is sprayed into the tunnel airstream by spray nozzles a great distance ahead of the body. The surface of the body is covered with an absorbent material (usually white blotter paper) upon which the dyed droplets impinge and are absorbed essentially upon contact. At the point of absorption, a permanent dye trace is obtained. The amount of dye obtained in a measured time interval can be determined by a colorimetric analysis of the blotter paper and converted into the amount of water that produced the dye trace. From such an analysis and known values of water content and droplet sizes, the impingement characteristics of a body can be determined.

Spray-cloud characteristics. - The pertinent characteristics of the spray cloud used for this study are summarized in the following table:

Volume-median droplet diameter, μ	Maximum droplet diameter, μ	Average water content, g/cu m
11.5	28	0.3
18.6	60	.6

The spatial variation of the liquid-water content in the cloud was about ±5 percent, whereas the reproducibility of the average liquid-water content from one spray exposure to the next was about ±6 percent.

The water contents listed in the preceding table were obtained with an aspirating device described in reference 3. Droplet-size measurements were made by relating the experimentally determined impingement characteristics for a body to the theoretical impingement data for the same bodies. For this study, small 36.5-percent Joukowski airfoils were used (unpublished theoretical data are available for this airfoil section).

The distribution of the droplet sizes from the volume-median size closely resembles a Langmuir D distribution (ref. 4). The accuracy of the volume-median droplet size is ±6 percent.

Blotter mounting. - Prior to each exposure to the spray cloud, a 2-inch-wide blotter of sufficient chordwise length to include the impingement region was rubber cemented to a vellum strip which, in turn, was cemented to the airfoil surface. The edges of the blotter were then taped to the airfoil surface (fig. 1). These mounting procedures are required to prevent lifting of the blotter from the airfoil surface by aerodynamic forces. After exposure to the spray cloud, the blotter and vellum are removed as a unit. The vellum and rubber cement then are removed carefully from the blotter.

Exposing models to spray cloud. - In order to minimize the evaporation of the dyed-water droplets, a saturated-air condition, as evidenced by a light condensation cloud in the test section, was obtained through the control of tunnel air temperature and the addition of steam to the airstream. With the tunnel air properly conditioned, the blotter-wrapped model was exposed to the dyed spray for the preset time interval. The blotter was then removed from the model. In these studies, the exposure time was 4 and 10 seconds for the large and small volume-median droplet sizes, respectively.

Colorimetric analysis. - In the colorimetric analysis of the dyed blotter (ref. 3), small segments were punched out of the blotters of the airfoil. Near the leading edge in the region of rapidly changing local impingement rate, 0.0625- by 1.0-inch segments were used to obtain the desired impingement accuracy, while elsewhere 0.125- by 1.0-inch segments were used. The dye was dissolved out of each segment in 5 milliliters of distilled water. The dye concentration of this solution was determined with a colorimeter by the amount of light of a suitable wavelength (520 mμ) that was transmitted through the solution. By using the concentration of the dye in the spray-tank supply, the local dye concentration on the blotter was then converted into the weight of water that impinged on the blotter segment during exposure to the spray cloud. The local impingement rate $\overline{W}_\beta$ (in terms of lb/(hr)(sq ft)) for a blotter segment is expressed in reference 3 as

$$\overline{W}_\beta = \frac{0.794\ Pb}{tc\ \Delta A_s}$$

Limits of impingement were obtained visually from the blotter by noting the rearmost significant trace of the dye deposit.

RESULTS

The aerodynamic and impingement characteristics of the truncated airfoils equipped with a flap are presented in terms of the local velocity ratio U/V_0 and the local impingement rate $\overline{W}_\beta$ as functions of the surface distance s measured from the zero chord point at the leading-edge region of the airfoil.

Velocity Distribution

Full-chord airfoil. - The velocity distribution over the full-chord airfoil for angles of attack of 0° and 4° is shown in figure 4 as a function of surface distance measured from the zero-chord point of the airfoil. At zero angle of attack, the local velocity ratio over both the upper and lower surfaces of the airfoil increases with surface distance, reaching U/V_0 values of about 1.22 on the upper surface and 1.16 on the lower surface. At a 4° angle of attack, the velocity ratio on the upper surface increases rapidly aft of the stagnation region and reaches a peak U/V_0 value of about 2.0 approximately 0.85 inch from the chord line. The velocity ratio then decreases until, at about 5 inches aft of the chord line, a relatively constant U/V_0 value of 1.4 is obtained over the instrumented portion of the airfoil. The velocity ratio over the lower surface at a 4° angle of attack increases with surface distance aft of the stagnation region and reaches a U/V_0 value of 1.03 at the end of the instrumented portion of the airfoil (s, 20.5 in.).

Truncated airfoils, flap deflected. - With increasing flap deflection, the velocity distribution over the surfaces of the truncated airfoils approach that of the full-chord airfoil. Because of the type of flap used and its location in a large protected or shadowed region at the end of the truncated airfoil (fig. 2(b)), large flap angles are required before the flap becomes effective and influences the velocity distribution on the airfoil. The actual projection of the lower surface of the flap beyond the original airfoil contours, however, did not exceed more than about 2 inches (airfoil thickness at max. thickness point was about 8.65 in.). The angle of flap deflection necessary to restore the velocity distribution to that of the full-chord airfoil is greater for the 30-percent-chord airfoil than for the 50-percent-chord airfoil, as shown in the following table:

Airfoil	Airfoil angle of attack, deg	Flap deflection angle, δ, deg
30-Percent chord	0	10.5
	4	22.0
50-Percent chord	0	9.5
	4	16.5

The velocity distributions obtained over the truncated airfoils using the preceding flap deflections are shown in figure 5 together with those for the full-chord airfoil. Generally good agreement is evident over most of the airfoil surfaces over which impingement data were obtained.

A small deviation in local velocity ratio is apparent, however, on the upper surface of the 30-percent-chord airfoil aft of the 13-inch station. The region over which these velocity-ratio discrepancies occur is generally not subject to impingement. For truncated chords less than 30 percent, this deviation will become more pronounced since it will occur nearer the leading edge, hence in the impingement region. Such an occurrence would establish a limit to the size the chord could be reduced and yet maintain a flow field in the impingement region substantially the same as that for the full-chord airfoil.

The simple mechanical flap used herein proved adequate to obtain substantially the same velocity distribution over the truncated airfoil surfaces as that for the full-chord airfoil. A problem may occur, however, with a truncated symmetrical airfoil at zero angle of attack. It is not known to what extent the flow field is altered about the leading-edge region of a symmetrical airfoil under these conditions. If the flow field is distorted for such an airfoil, then the mechanical flap used herein would prove ineffective in restoring the full-chord velocity distribution. However, a double-split flap, similar to a wing dive brake, possibly could be used. If such a double-split flap is inadequate, an air flow source or sink at the end of the truncated airfoil could be used effectively. Such a device (jet flap) could be used at all angles of attack, thereby replacing the mechanical flap.

Truncated airfoils, flap undeflected. - The local velocity ratios for the 50- and 30-percent-chord airfoils with flap undeflected are shown in figure 6 as a function of surface distance measured from the chord line and for angles of attack of 0° and 4°. Also shown for comparative purposes are the velocity distribution curves for the full-chord airfoil. The data shown in figure 6 indicate that the truncated airfoils

with flap undeflected operate at decreased lift coefficients. These phenomenon are evident from the decrease in the local U/V_0 values on the upper surface and the increase in U/V_0 values on the lower surface over those of the full-chord airfoil. Although large differences in U/V_0 values occur for the truncated airfoils when compared with those for the full-chord airfoil, only minor differences in U/V_0 values are apparent between the 30- and 50-percent-chord airfoils.

Impingement

Full-chord airfoil. - The local rates of water impingement $\overline{W}_\beta$ (lb/(hr)(sq ft)) for the full-chord airfoil as a function of surface distance measured from the chord line are shown in figure 7 for angles of attack of 0° and 4°. The higher values of $\overline{W}_\beta$ are for a volume-median droplet size of 18.6 microns, while the lower values of $\overline{W}_\beta$ are for a volume-median droplet size of 11.5 microns. The maximum rate of impingement occurs between the air stagnation point and the foremost point of the airfoil. (The foremost point of an airfoil is not necessarily coincident with the zero-chord point, ref. 5.) Aft of the maximum W_β value, the rate of impingement decreases on both upper and lower surfaces until the limit of impingement is reached ($\overline{W}_\beta = 0$).

At zero angle of attack, the impingement, because of the airfoil camber, extends over a somewhat greater distance on the upper surface than on the lower surface. Approximately 60 percent of the water collected by the airfoil impinges on the upper surface, whereas only 40 percent impinges on the lower surface. At a 4° angle of attack, about 85 percent of the water collected by the airfoil impinges on the lower surface, whereas only 15 percent of the water impinges on the upper surface. The impingement limits for the full-chord airfoil are summarized in the following table:

Angle of attack, deg	Volume median droplet size, μ	Full-chord impingement limits, in.	
		Upper surface	Lower surface
0	11.5	2.9	1.4
	18.6	7.2	5.0
4	11.5	0.7	5.0
	18.6	2.2	14.0

Truncated airfoils, flap deflected. - With the flap deflected as indicated in the preceding table on flap deflection angle, the impingement characteristics of the truncated airfoils (local impingement rates and limits of impingement) are similar in all respects to those of the full-chord airfoil. The local impingement rates of the truncated airfoils with flap deflected and the $\bar{W}_\beta$ curve for the full-chord airfoil are shown in figure 8 as a function of surface distance for angles of attack of 0° and 4°. Good agreement for the various airfoil configurations is apparent. The small deviations of U/V_0 values on the upper surface for the 30-percent-chord airfoil have no apparent effect on the limit of impingement on the upper surface or on the $\bar{W}_\beta$ values. It is of interest to note also that, although the projected frontal height of the 30-percent-chord airfoil is smaller than that of the full-chord airfoil, this factor (for the model studied) has no apparent effect on the $\bar{W}_\beta$ values. Indiscriminate reductions in the chord would result in decreases in projected frontal height of the airfoil which, coupled with large velocity deviations on the upper surface, very likely could affect the airfoil impingement characteristics. It is not implied, however, that the 30-percent-chord truncated flapped airfoil studied herein is the minimum chord ratio for which impingement characteristics similar to those of the full-chord airfoil can be obtained.

Truncated airfoils, flap undeflected. - The $\bar{W}_\beta$ values of the truncated airfoils with flap undeflected are shown in figure 9 as a function of surface distance for angles of attack of 0° and 4°. For comparative purposes, the $\bar{W}_\beta$ curves for the full-chord airfoil are also shown. In general, the $\bar{W}_\beta$ values for the truncated airfoils are shifted toward the upper surface from those of the full-chord airfoil, indicative of an effectively lower angle of attack. This shift in the local-impingement-rate values correlates with the results of the velocity-distribution study, discussed previously, which also showed the truncated airfoil to be effectively operating at a lower lift coefficient if the flap was undeflected. At zero angle of attack, the shift in the $\bar{W}_\beta$ values for the truncated airfoils is not as apparent as at a 4° angle of attack. In comparison with the 50-percent-chord airfoil, the 30-percent-chord airfoil shows a somewhat greater shift in the $\bar{W}_\beta$ values at 4° angle of attack; however, this greater shift can also be correlated with the velocity-distribution data that show a similar trend. The locations of the maximum $\bar{W}_\beta$ values for the truncated airfoils are nearer to the foremost point of the airfoil than those for the full-chord airfoil.

The total water catch (obtained by integration under the $\bar{W}_\beta$ curve) for the truncated airfoils with flap undeflected is generally greater (as much as 10 percent) at zero angle of attack than that obtained for the full-chord airfoil. At a 4° angle of attack, however, the total

water catch for the truncated airfoils with flap undeflected is generally less (as much as 35 percent for the 30-percent-chord airfoil) than that for the full-chord airfoil.

In general, at zero angle of attack, the truncated airfoils with flap undeflected show an increase in total water catch of 9 to 26 percent on the upper surface and a decrease of 30 to 16 percent on the lower surface for volume-median droplet sizes of 11.5 and 18.6 microns, respectively, compared with that for the full-chord airfoil. At a 4° angle of attack, the truncated airfoils with flap undeflected have an increase in total water catch of as much as 69 percent on the upper surface and a decrease of as much as 46 percent on the lower surface (volume-median droplet size, 18.6 μ) compared with that of the full-chord airfoil. Similar changes in total water catch on the upper and lower surfaces of the truncated airfoils occur with the smaller volume-median droplet size. A comparison of the percentage of water caught on the upper and lower surfaces of the truncated airfoils with that of the full-chord airfoils is shown in the following table:

Angle of attack, deg	Total water catch, percent					
	30-Percent-chord airfoil		50-Percent-chord airfoil		Full-chord airfoil	
	Upper surface	Lower surface	Upper surface	Lower surface	Upper surface	Lower surface
0	0.70	0.30	0.70	0.30	0.60	0.40
4	.37	.63	.30	.70	.15	.85

The limit of impingement on the truncated airfoils also deviates from that of the full-chord airfoil. On the upper surface, the impingement extends further aft on the truncated airfoils; while, on the lower surface, the impingement limit is decreased compared with the values on the full-chord airfoil. The following table summarizes the impingement limits measured for the truncated airfoils with flap undeflected and for the full-chord airfoil:

Angle of attack, deg	Volume median droplet size, μ	Impingement limits, in.					
		30-Percent chord airfoil		50-Percent-chord airfoil		Full-chord airfoil	
		Upper surface	Lower surface	Upper surface	Lower surface	Upper surface	Lower surface
0	11.5	3.0	1.1	2.8	1.0	2.9	1.4
	18.6	8.9	4.7	9.3	5.4	7.2	5.0
4	11.5	1.4	2.1	1.2	2.3	0.7	5.0
	18.6	6.7	9.5	5.1	10.0	2.2	14.0

DISCUSSION

The use of truncated flapped airfoils does not eliminate entirely scale-model icing problems. Problems involving aerodynamic penalties caused by icing and those involving tunnel limitations of airspeed and pressure altitude cannot be solved by these airfoils. Fortunately, these limitations are not serious for many aircraft, since icing in many cases may be encountered only at low airspeeds and at relatively low altitudes (ascent and descent conditions). Various aspects in the utilization of truncated flapped airfoils for studies involving impingement, icing characteristics, and heat transfer are discussed in the following sections.

Impingement

In extrapolating impingement data obtained with truncated flapped airfoils to conditions beyond the range of those covered in tests, the modified inertia parameter K_0 may be used. This parameter contains a body dimension that for airfoils is the chord length. In plotting the impingement data obtained from truncated flapped airfoils, the full-chord dimension should be used in calculating K_0 rather than the truncated chord.

Use of a flap on either truncated or full-chord airfoils may be useful also in reducing tunnel-wall interference effects. For large airfoil models, the effect of the tunnel walls generally is to increase the effective angle of attack of the airfoil (a higher lift coefficient for the same geometric angle of attack). This effect will also affect the impingement on the airfoil since less impingement will occur on the upper surface and more impingement on the lower surface of the airfoil compared with that encountered in flight at the same geometric angle of attack (neglecting induced effects). By means of a flap, the tunnel

flow field and, hence, the impingement about an airfoil can be adjusted to represent more nearly those encountered in flight.

Ice Formations

One of the problems in scale-model icing theory is the prediction of the shape and size of an ice formation. This problem is extremely complex and involves simultaneous scaling of impingement, aerodynamic, and thermal considerations that are not readily solved by existing methods. By the use of truncated flapped airfoils, the ice shape and size can be obtained for full-scale airfoils for a wide range of equivalent full-chord airfoils. In addition, the aerodynamic forces involved in shedding ice formations during operation of a cyclic de-icing system can be studied with full scale leading-edge section over a wide range of airfoil chord sizes.

4100

Heat Transfer

The heat-transfer parameters obtained with truncated flapped airfoils can be applied directly to the evaluation of an aircraft wing-icing-protection system since the local velocities, impingement rates, heat-transfer coefficients, Reynolds number, ice shape and location, and physical dimensions of the system are the same as those for a full-scale system. The ability to conduct such tests without scaling the data and model configuration should provide large benefits from the point of view of reduced flight-evaluation studies, since all associated equipment required for a full-scale system (including valves, ducting, automatic controls, etc) can be evaluated while the icing-protection system is under test.

Limitations to Use of Truncated Flapped Airfoils

The size to which an airfoil can be truncated depends on several factors. In general, the model must be of sufficient size to contain the desired icing-protection system. This size is determined by the limit of droplet impingement or the rearward extent of the protection system. The latter may be coincident with the impingement limit (e.g., a pneumatic de-icer boot need not extend beyond the impingement limits for the design condition) or may extend beyond the impingement limit (cyclic de-icing system that must consider run-back refreezing or secondary cycling regions). These rearward extents of the protection system will, or course, depend also on the physical size of the component since the impingement parameters are dependent on a body dimension (usually chord length). For large airfoils, for example, an icing-protection system may only extend rearward 10 percent of the chord

size; whereas, for a smaller airfoil, the rearward extent may be as far as the front spar of the wing or about 20 percent of the chord. For airfoils with thickness ratios of 4 to 6 percent and at an angle of attack, the rearward extent based on impingement considerations alone could be as much as 50 or 100 percent on the lower surface; however, for practical construction reasons, the rearward extent of the protection system is often only 15 to 20 percent of the chord.

A truncated airfoil consisting of 10 percent of the full chord plus a flap may not prove feasible. It is pointed out in the RESULTS section that, as the percentage of full chord is reduced, the flow field on the upper surface is subject to deviations from that obtained with a full-chord airfoil. The selection of the minimum size of the truncated airfoil is therefore a compromise dictated by the desired protection system, the impingement limits, the airfoil shape, and the degree of full-scale air flow simulation desired over the leading-edge region. It should be noted that, while the air flow restoration over the 30-percent-chord airfoil equipped with a flap was good, other airfoil shapes may not necessarily yield as good results. For airfoils truncated more than 50 percent of chord, brief studies to determine the velocity distribution are required in order to establish the optimum chord size to which a particular airfoil can be shortened and still maintain the velocity distribution of the full-chord airfoil.

CONCLUDING REMARKS

The results of a study of the effect of the velocity distribution and impingement characteristics of truncating the chord of an NACA 65_1-212 airfoil section with and without a trailing-edge flap may be summarized as follows:

1. The velocity distributions in the impingement region for the airfoils truncated at 50 and 30 percent of chord were substantially the same as those for the full-chord airfoil when the trailing-edge flap was sufficiently deflected.

2. With the trailing-edge flap on the truncated airfoil deflected so that the local velocity distribution in the impingement region was substantially the same as that for the full-chord airfoil, the local impingement rates and the limits of impingement for the truncated and full-chord airfoils were the same.

3. With the trailing-edge flap undeflected, the velocity distribution and the local impingement rate on the surfaces of the truncated airfoils were substantially altered from those of the full-chord airfoil. In general, the truncated airfoil chord with flap undeflected resulted

in a lower effective angle of attack that caused more impingement on the upper surface and less impingement on the lower surface of the truncated airfoil compared with that of the full-chord airfoil at the same geometric angle of attack.

Use of flapped truncated airfoils can extend the range of usefulness of wind tunnels for full-scale impingement and icing studies.

Lewis Flight Propulsion Laboratory
National Advisory Committee for Aeronautics
Cleveland, Ohio, May 15, 1956

REFERENCES

1. Hauger, H. H., and Englar, K. G.: Analysis of Model Testing in an Icing Wind Tunnel. Rep. No. SM 14993, Douglas Aircraft Co., Inc., May 14, 1954.

2. Sibley, P. J., and Smith, R. E., Jr.: Model Testing in an Icing Wind Tunnel. Rep. No. LR 10981, Lockheed Aircraft Cor., Oct. 14, 1955.

3. von Glahn, Uwe H., Gelder, Thomas F., and Smyers, William H., Jr.: A Dye-Tracer Technique for Experimentally Obtaining Impingement Characteristics of Arbitrary Bodies and a Method for Determining Droplet Size Distribution. NACA TN 3338, 1955.

4. Langmuir, Irving, and Blodgett, Katherine B.: A Mathematical Investigation of Water Droplet Trajectories. Tech. Rep. No. 5418, Air Materiel Command, AAF, Feb. 28, 1946. (Contract No. W-33-038-ac-9151 with General Electric Co.)

5. Abbott, Ira H., von Doenhoff, Albert E., and Stivers, Louis S., Jr.: Summary of Airfoil Data. NACA Rep. 824, 1945. (Supersedes NACA WR L-560.)

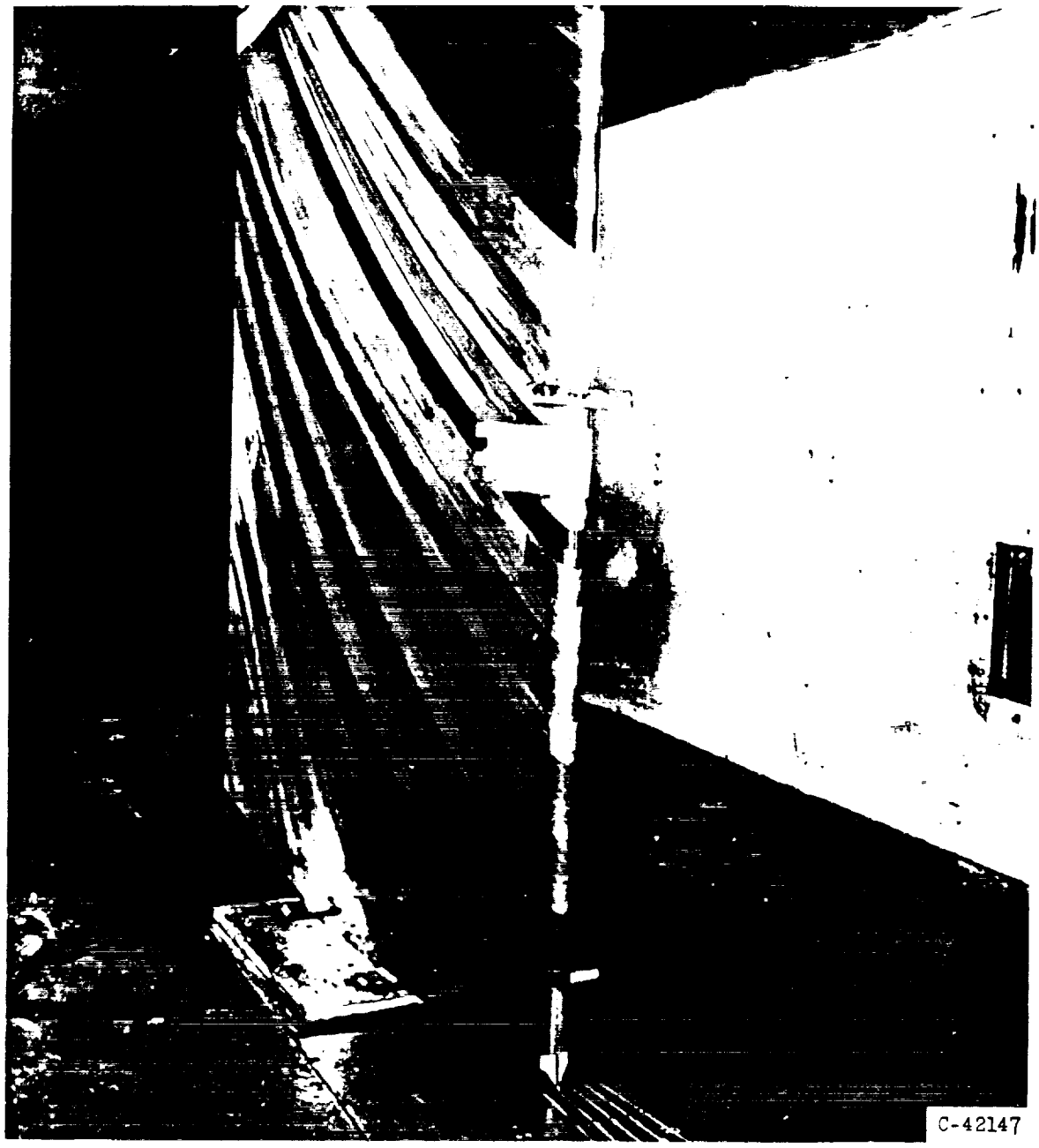

Figure 1. - Installation of NACA 65_1-212 airfoil model (6 ft.-chord) in icing tunnel.

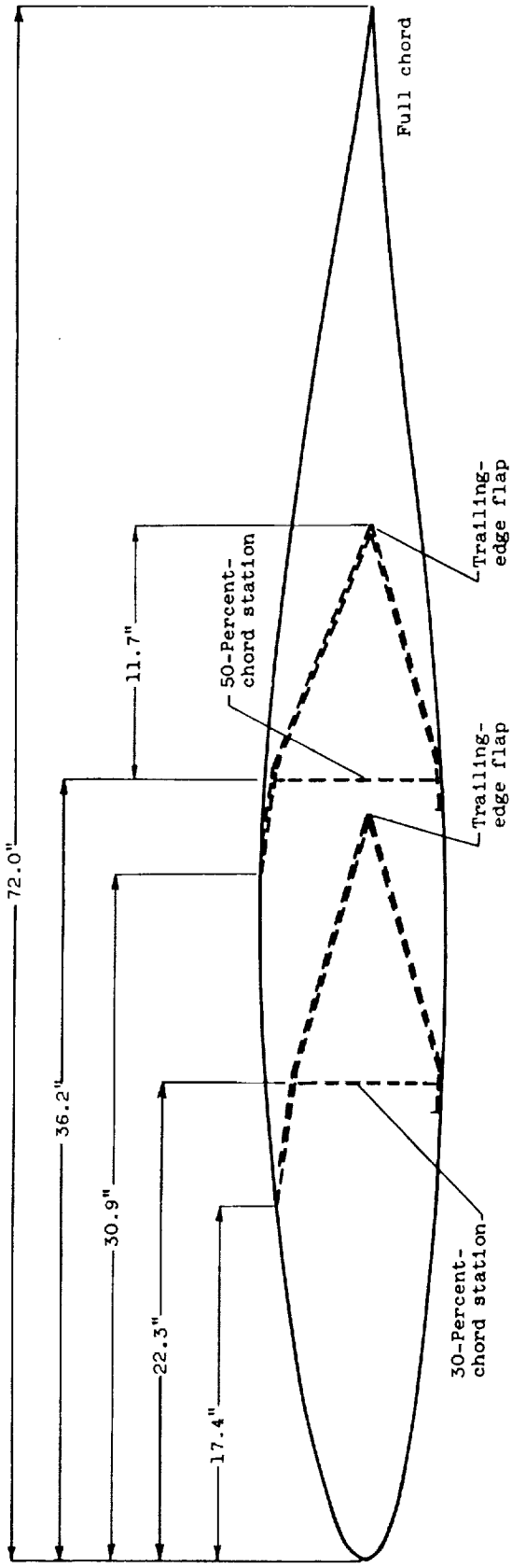

(a) Cross section of truncated and full-chord airfoils.

Figure 2. - Location of trailing-edge flaps on airfoils.

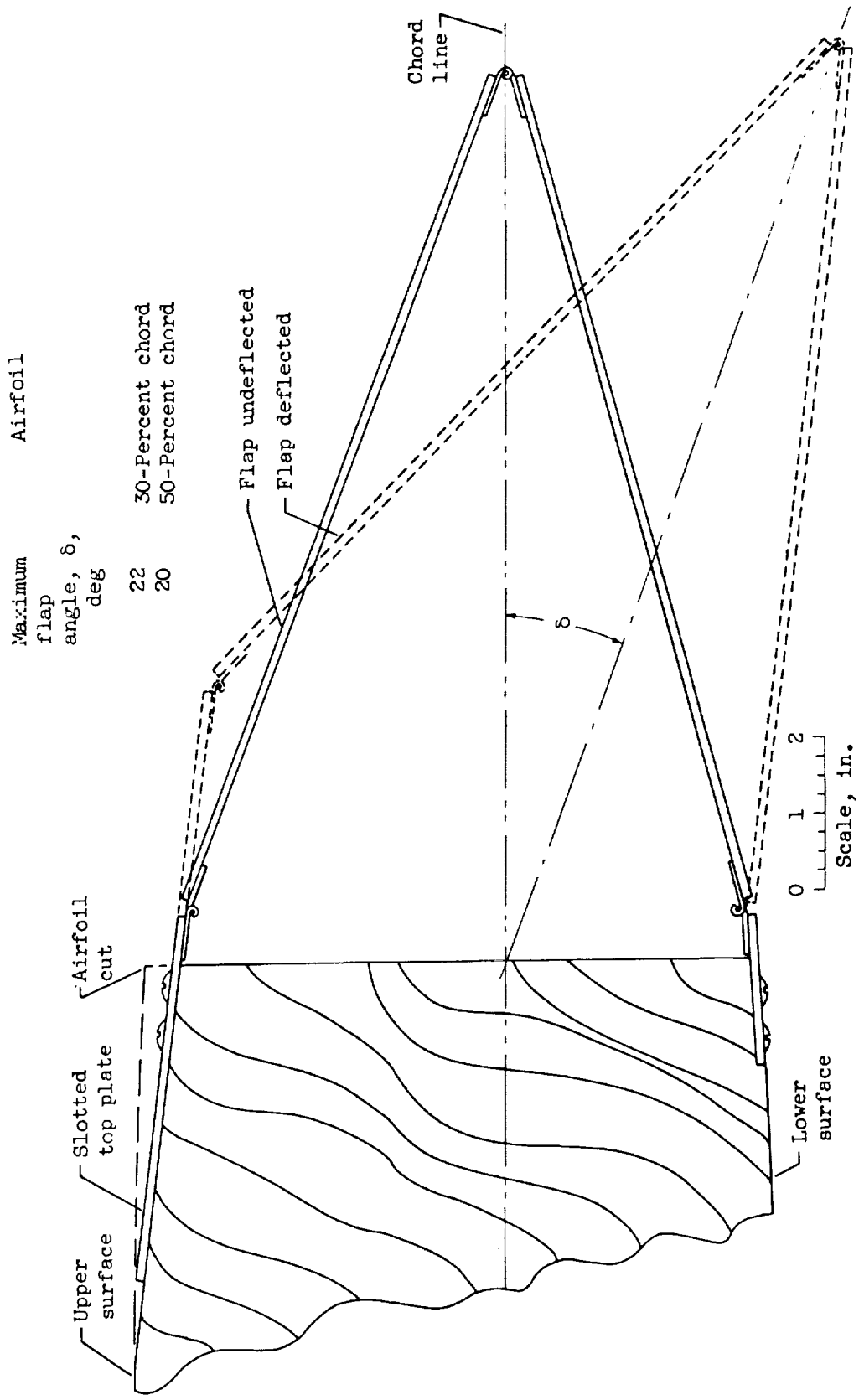

(b) Flap details.

Figure 2. - Concluded. Location of trailing-edge flaps on airfoils.

Figure 3. - Installation of 30-percent-chord truncated airfoil with trailing-edge flap in icing tunnel.

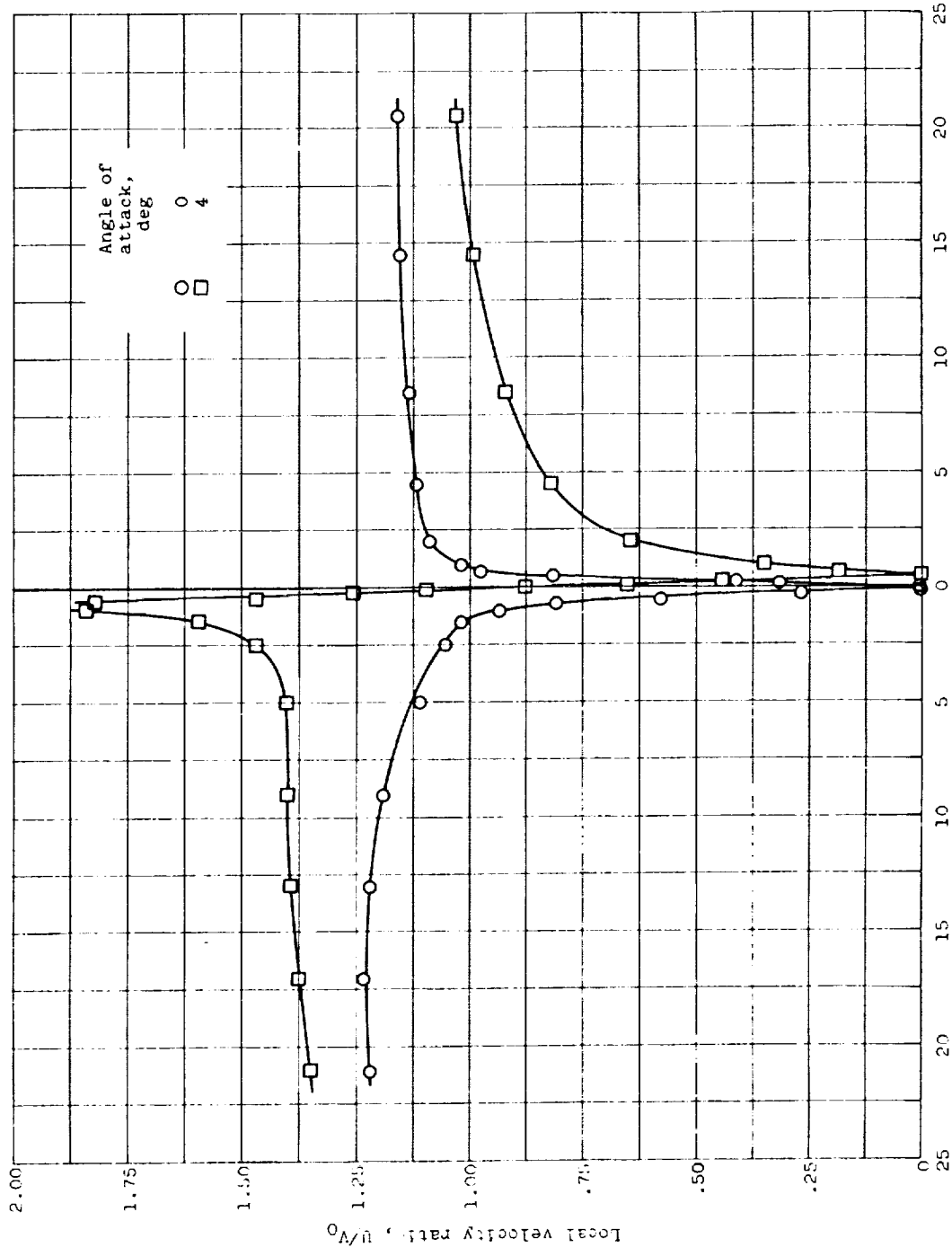

Figure 4. - Velocity distribution over leading-edge region of full-chord NACA 65_1-212 airfoil. Airspeed, 156 knots.

4100

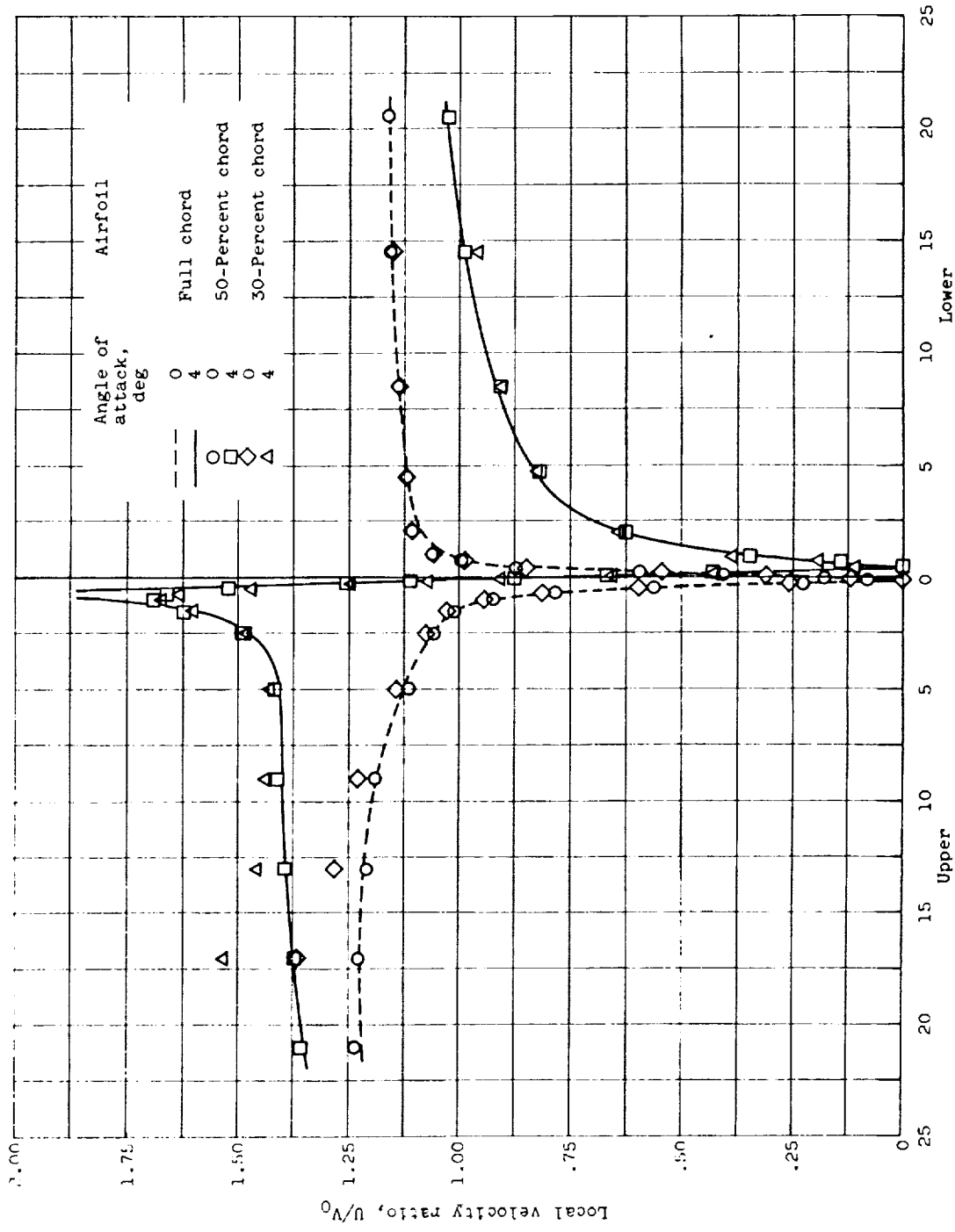

Figure 5. - Comparison of velocity distribution for 30- and 50-percent-chord NACA 65_1-212 airfoil models with that for full-chord model. Flap deflected; airspeed, 156 knots.

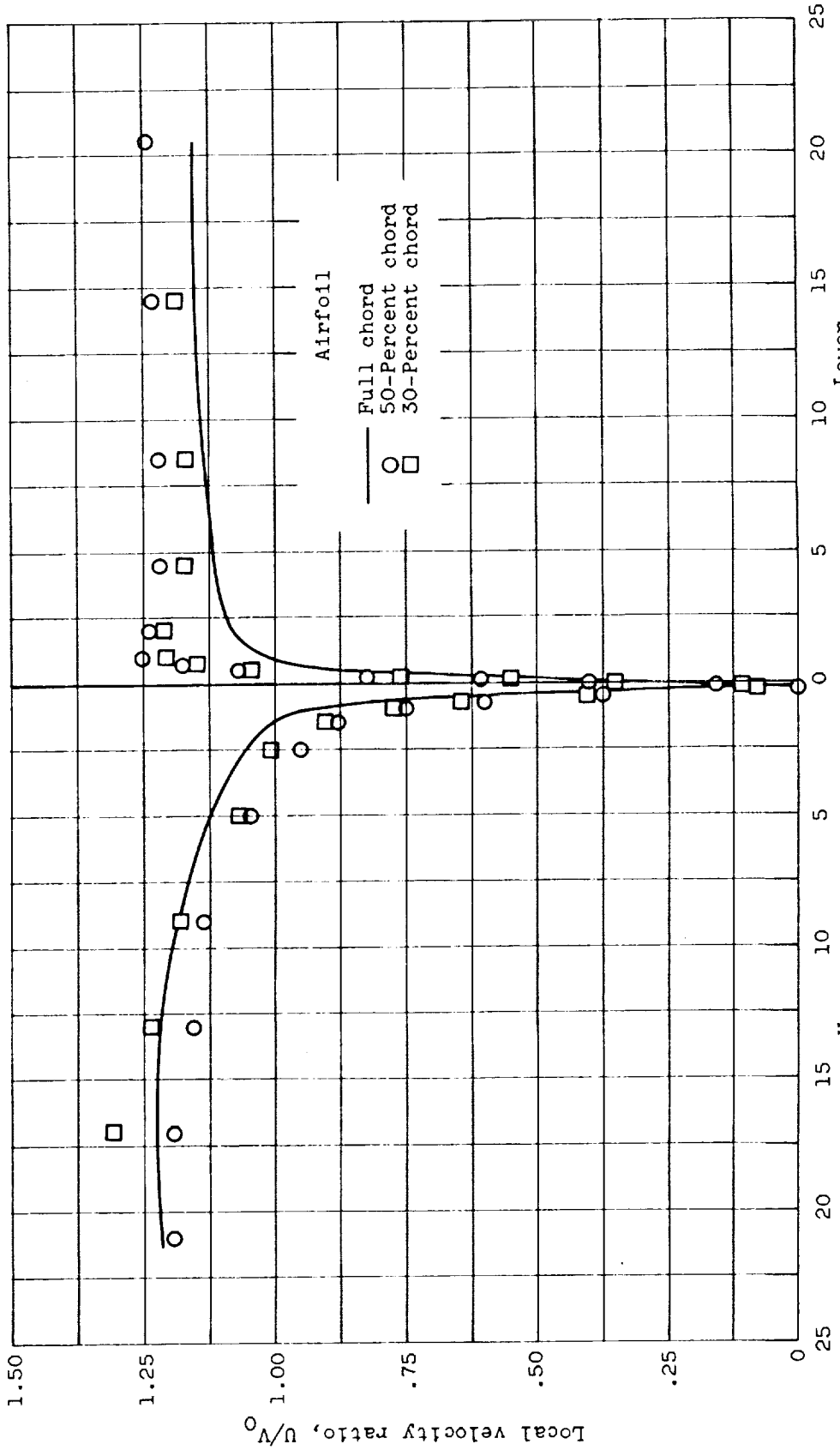

(a) Angle of attack, 0°.

Figure 6. - Comparison of velocity distribution for 30- and 50-percent-chord NACA 65_1-212 airfoil models with that for full-chord model. Flap undeflected; airspeed, 156 knots.

4100

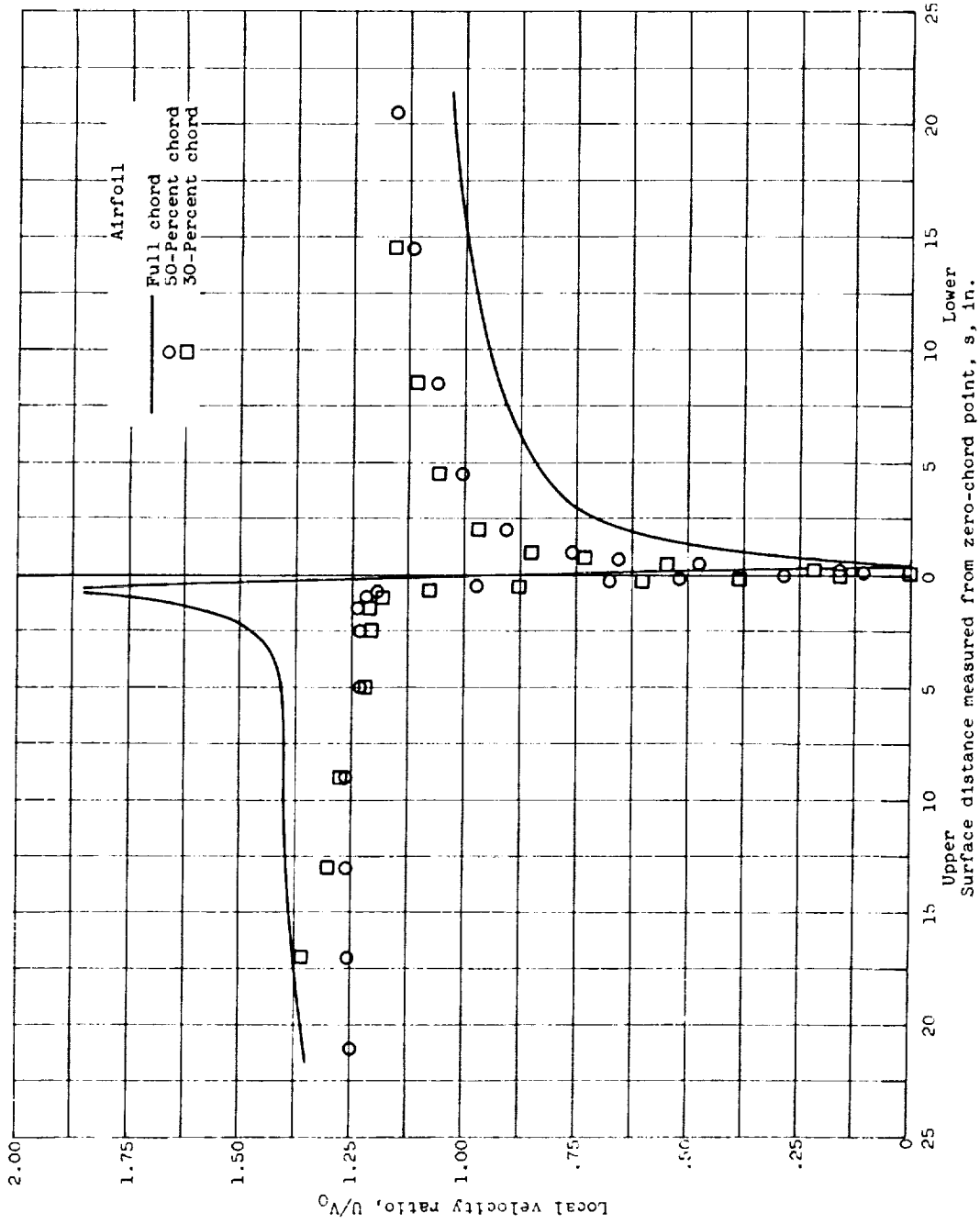

(b) Angle of attack, 4°.

Figure 6. - Concluded. Comparison of velocity distribution for 30- and 50-percent-chord NACA 65_1-212 airfoil models with that for full-chord model. Flap undeflected; airspeed, 156 knots.

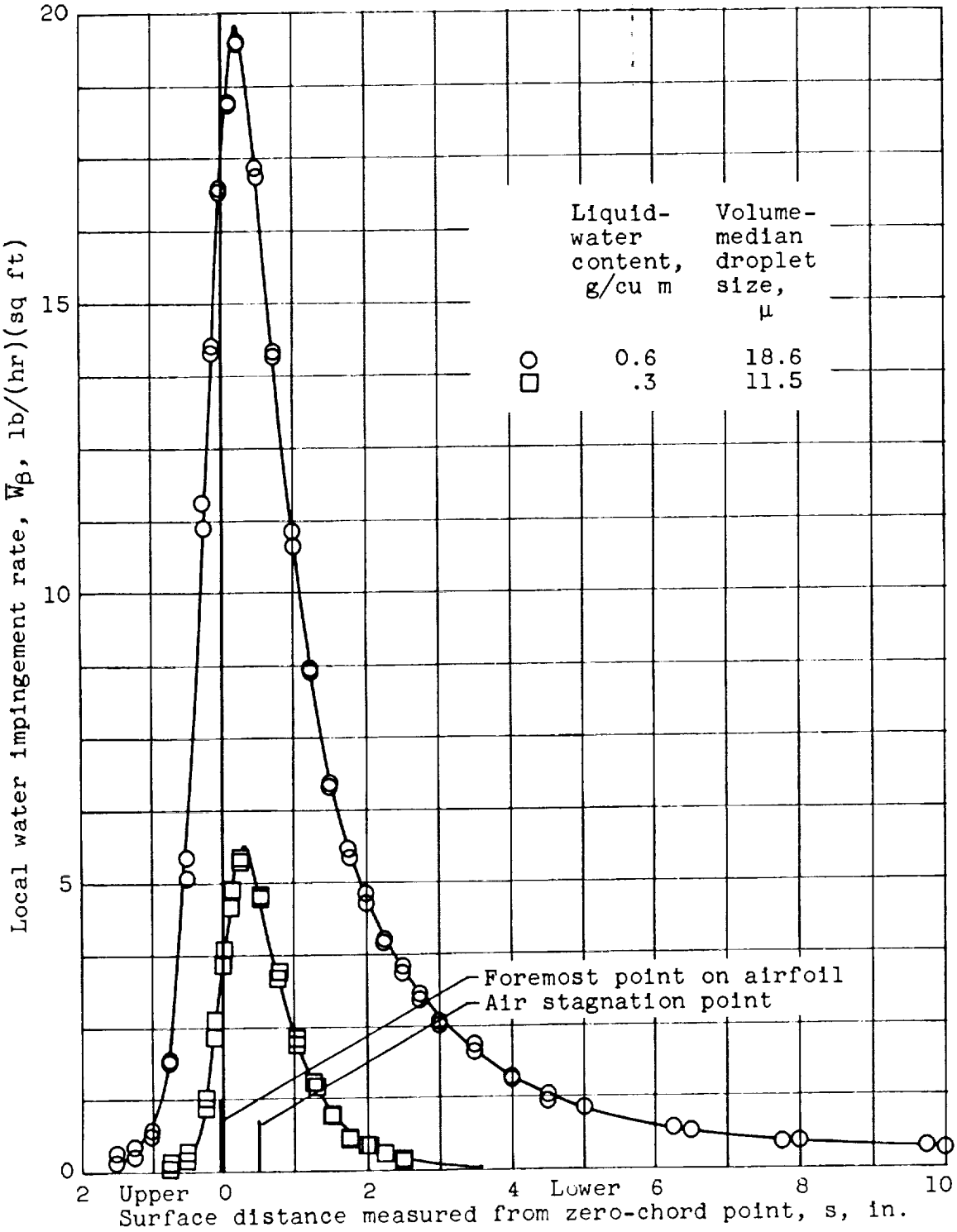

(b) Angle of attack, 4°.

Figure 7. - Concluded. Local water impingement rate on surface of full-chord NACA 65_1-212 airfoil. Airspeed, 156 knots.

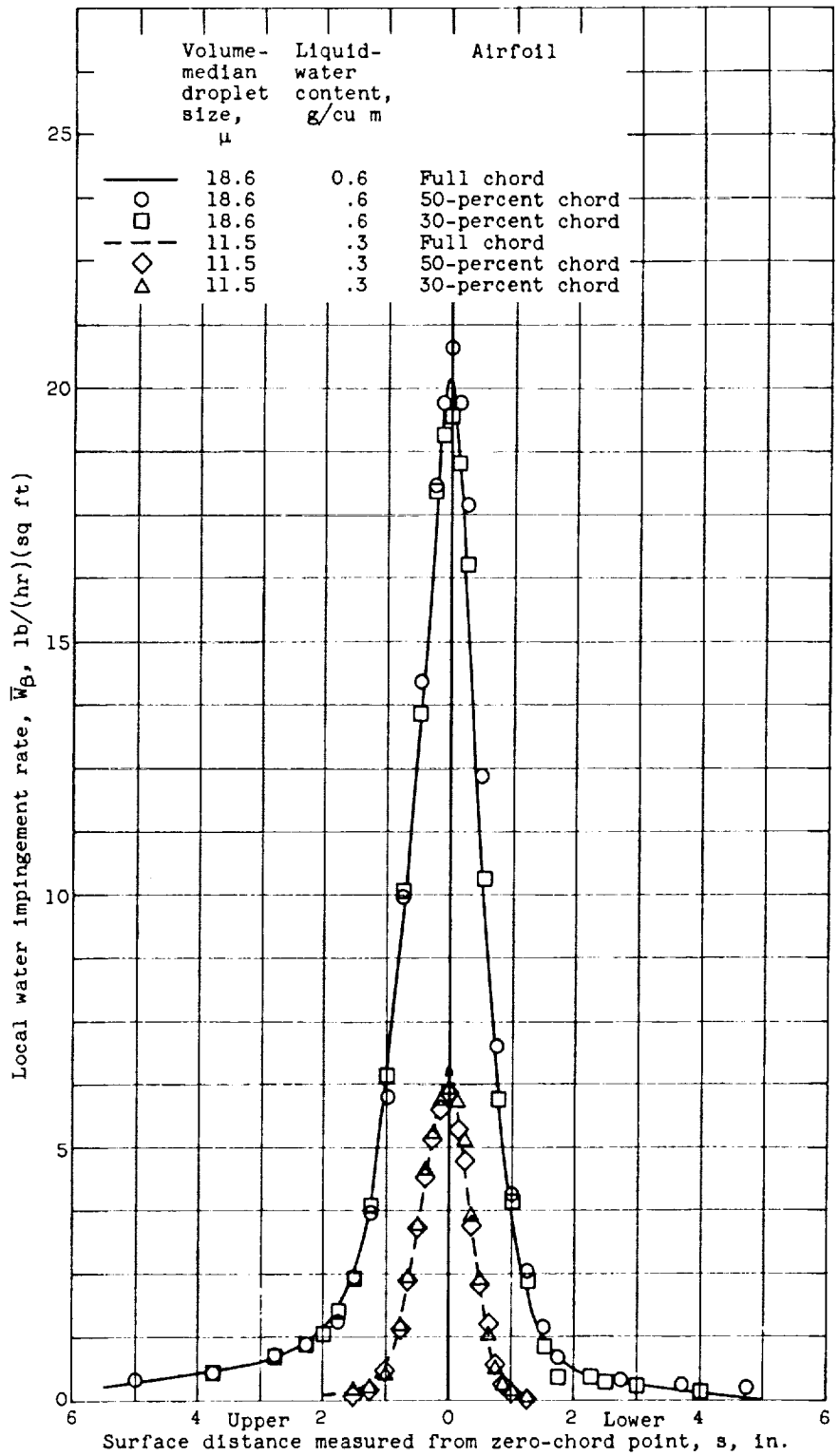

(a) Angle of attack, 0°.

Figure 8. - Comparison of local water impingement rate on surfaces of 30- and 50-percent-chord truncated NACA 65_1-212 airfoils with that for full-chord model. Flap deflected; airspeed, 156 knots.

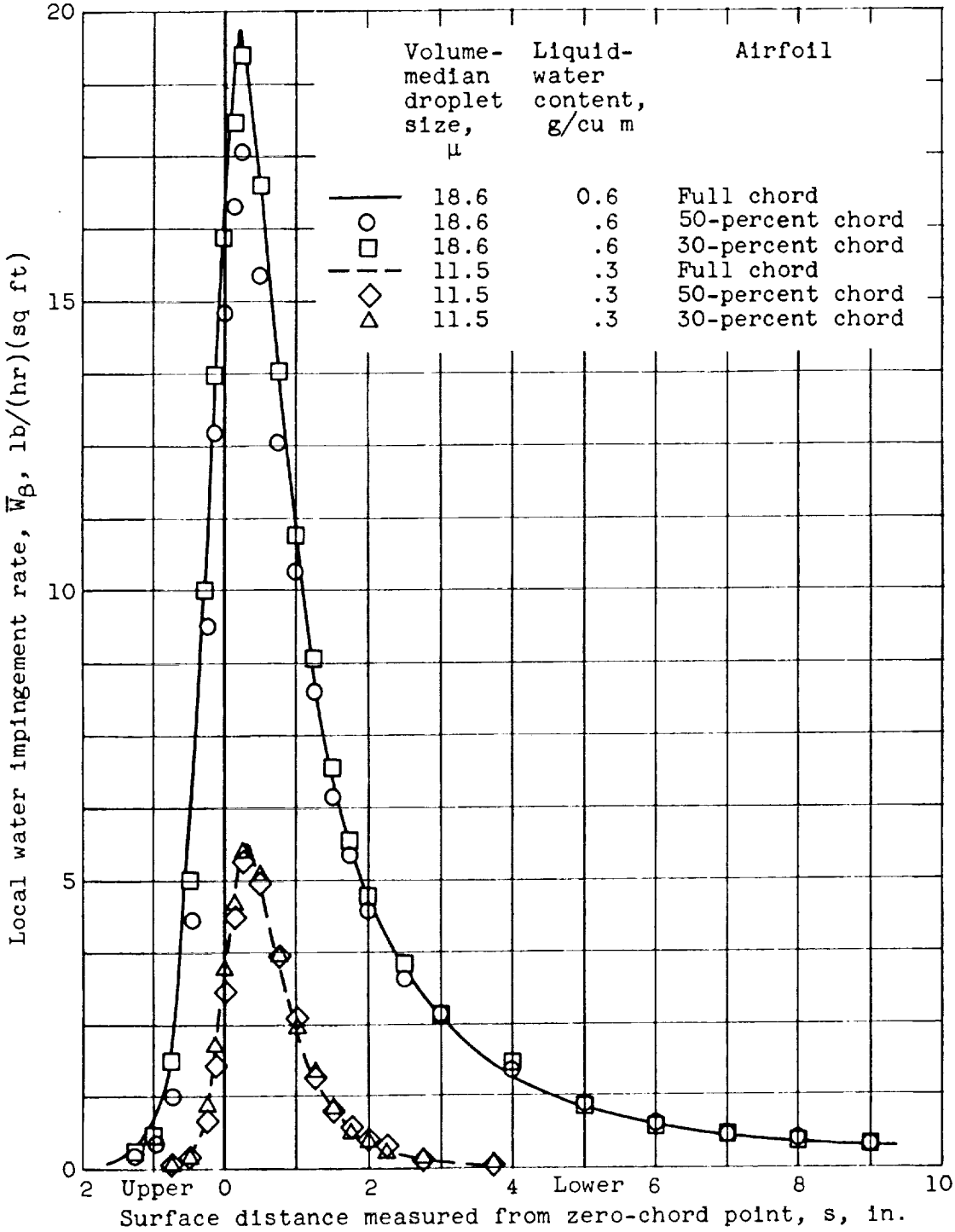

(b) Angle of attack, 4°.

Figure 8. - Concluded. Comparison of local water impingement rate on surfaces of 30- and 50-percent-chord truncated NACA 65_1-212 airfoils with that for full-chord model. Flap deflected; airspeed, 156 knots.

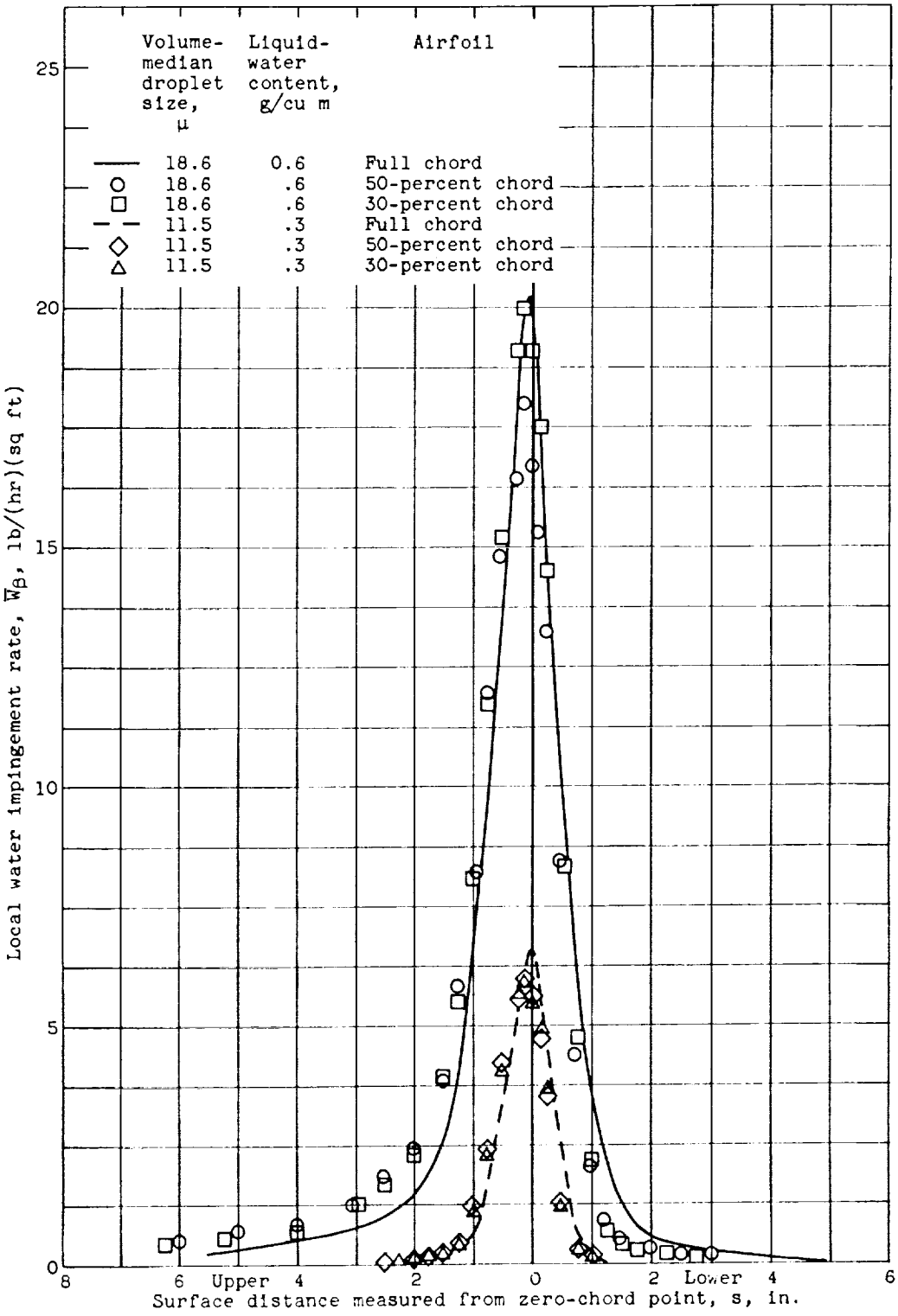

(a) Angle of attack, 0°.

Figure 9. - Comparison of local water impingement rate on surfaces of 30- and 50-percent-chord truncated NACA 65_1-212 airfoils with that for full-chord model. Flap undeflected; airspeed, 156 knots.

4100

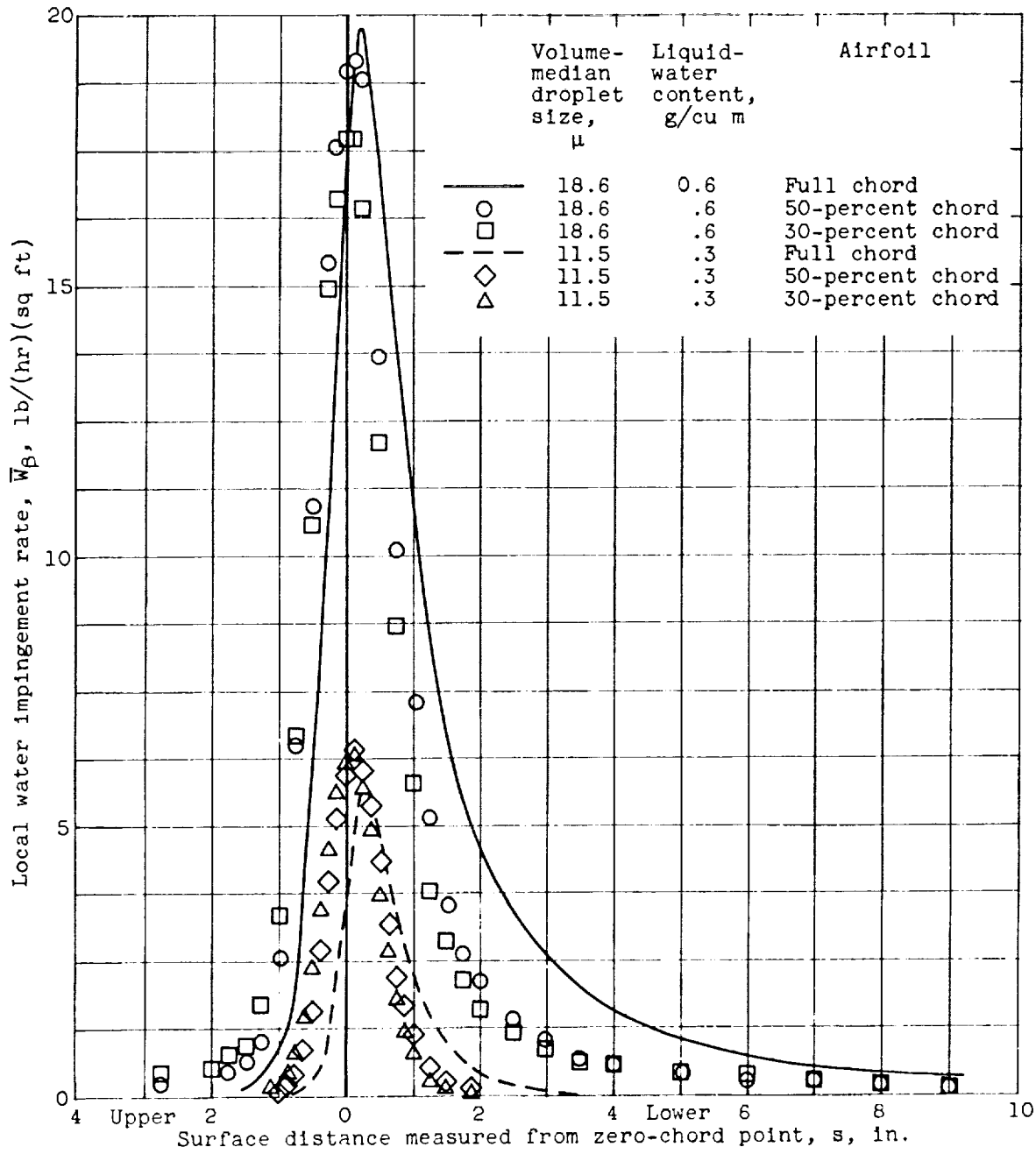

(b) Angle of attack, 4°.

Figure 9. - Concluded. Comparison of local water impingement rate on surfaces of 30- and 50-percent truncated NACA 65_1-212 airfoils with that for full-chord model. Flap undeflected; airspeed, 156 knots.